Development of a generic high-throughput screening assay for profiling snake venom protease activity after high-resolution chromatographic fractionation

Neumann, Coleen; Slagboom, Julien; Somsen, Govert W.; Vonk, Freek; Casewell, Nicholas R.; Cardoso, Carmen L.; Kool, Jeroen

published in
Toxicon
2020

DOI (link to publisher)
10.1016/j.toxicon.2020.02.015

document version
Publisher's PDF, also known as Version of record

Toxicon 178 (2020) 61–68

Contents lists available at ScienceDirect

Toxicon

journal homepage: http://www.elsevier.com/locate/toxicon

Development of a generic high-throughput screening assay for profiling snake venom protease activity after high-resolution chromatographic fractionation

Coleen Neumann [a], Julien Slagboom [a], Govert W. Somsen [a], Freek Vonk [b], Nicholas R. Casewell [c], Carmen L. Cardoso [d], Jeroen Kool [a,*]

[a] Division of BioAnalytical Chemistry, Department of Chemistry and Pharmaceutical Sciences, Amsterdam Institute of Molecules, Medicines and Systems, Vrije Universiteit Amsterdam, Amsterdam, the Netherlands
[b] Naturalis Biodiversity Center, 2333 CR, Leiden, the Netherlands
[c] Centre for Snakebite Research & Interventions, Liverpool School of Tropical Medicine, Pembroke Place, Liverpool, L3 5QA, UK
[d] Departamento de Química, Grupo de Cromatografia de Bioafinidade e Produtos Naturais - Faculdade de Filosofia, Ciências e Letras de Ribeirão Preto - Universidade de São Paulo, Brazil

ARTICLE INFO

Keywords:
Rhodamine-110 bis-(p-tosyl-L-glycyl-L-prolyl-L-arginine amide) peptide substrate
Casein-FITC substrate
Nanofractionation
Snake venom protease
Fluorescence bioassay
Vipers
Toxins
Snakebite

ABSTRACT

Snakebites cause upwards of 1.8 million envenomings, 138,000 deaths and 500,000 cases of long term morbidity each year. Viper snake venoms (family Viperidae) generally contain a high proportion of proteases which can cause devastating effects such as hemorrhage, coagulopathy, edema, necrosis, and severe pain, in envenomed victims. In this study, analytical techniques were combined with enzymatic assays to develop a novel method for the detection of snake venom protease activity by using rhodamine-110-peptide substrate. In the so called at-line nanofractionation set up, crude venoms were first separated with reversed phase liquid chromatography, after which fractions were collected onto 384-well plates. Protease activity assays were then performed in the 384-well plates and bioassay chromatograms were constructed revealing protease activity. Parallel obtained UV absorbance, MS and proteomics data from a previous study facilitated toxin identification. The application of the rhodamine-110-peptide substrate assay showed significantly greater sensitivity compared to prior assays using casein-FITC as the substrate. Moreover, cross referencing UV and MS data and resulted in the detection of a number of tentative proteases suspected to exhibit protease activity, including snake venom serine proteases from *Calloselasma rhodostoma* and *Daboia russelli* venom and a snake venom metalloproteinase from the venom of *Echis ocellatus*. Our data demonstrate that his methodology can be a useful tool for selectively identifying snake venom proteases, and can be applied to provide a better understanding of protease-induced pathologies and the development of novel therapeutics for treating snakebite.

1. Introduction

Proteases are key enzymes that perform myriad functions in various physiological systems, including those relating to digestion, hemostasis, apoptosis, signal transduction, blood coagulation, and immune responses. Snake venoms are rich in enzymatic proteins with diverse specificity and activity (Hedstrom, 2002; Schauperl et al., 2015). These, and other non-enzymatic venom components, exhibit complex evolutionary histories, which have resulted in snake venoms containing a complex mixture of numerous protein/peptide components that are used for prey capture (Fry et al., 2008). Thus, the composition of snake venom —even within a species— is often highly variable and is influenced by any number of external factors, such as the snake's age or diet, geographical location, or the season of the year (Chippaux et al., 1991).

In snake venom, particularly those of vipers, proteases are key toxin types involved in causing severe pathologies such as hemorrhage, coagulopathy, edema, and intense local pain at the bite site (Kini and Koh, 2016). These various clinical signs can in part be attributed to the activity of snake venom metalloproteases (SVMPs), which destroy capillary blood cells and surrounding tissues, the basement membrane, and vascular and muscular tissues (Arpitha et al., 2017; Gutiérrez et al., 2016). Another class of relevant snake venom protease toxins, the snake

* Corresponding author.
E-mail address: j.kool@vu.nl (J. Kool).

https://doi.org/10.1016/j.toxicon.2020.02.015
Received 27 November 2019; Received in revised form 22 January 2020; Accepted 11 February 2020
Available online 26 February 2020

venom serine proteases (SVSPs), interfere with blood coagulation by activating coagulation pathways and exerting fibrinogenolytic activities, resulting in the depletion of fibrinogen, and thus contributing to a life threatening pathology called venom induced consumption coagulopathy (Kini, 2005). If left untreated, the hemotoxic effects of these snake venom proteases, along with other venom toxins, can cause extravasation, catastrophic losses of blood pressure and extensive local tissue necrosis.

Snakebite is a neglected tropical disease that affects millions of people each year, and results in more than 100,000 deaths annually and 400,000 injuries (Gutiérrez et al., 2017). Snakebite is treated via the use of intravenously delivered polyclonal antibody therapies known as antivenom. However, due to a variety of biological and socioeconomic factors, including poor cross-snake species efficacy (Casewell et al., 2014), high cost and low availability (Gutiérrez et al., 2017), antivenom accessibility is often deficient in many of the impoverished rural communities that face the highest risks of snakebite. Understanding the function and variation of snake venom components is crucial to developing more effective and affordable snakebite treatments, in addition to uncovering potentially therapeutic compounds (Slagboom et al., 2017). For the above reasons, inhibiting snake venom protease activity is of particular importance because these enzymes are often responsible for causing severe, often life-threatening, pathologies.

To better understand the composition and function of snake venoms, we have developed an analytical “nanofractionation” platform capable of separating and fractionating venoms, and correlating observed bioactivity of fractions - using custom bioassays - with parallel acquired accurate masses of the venom components (Mladic et al., 2017; Mladic et al., 2016; Mladic et al., 2015). In this study, we sought to employ our nanofractionation platform for the characterization of proteases in snake venom. For that purpose, we developed a new generic fluorescence bioassay based on a rhodamine substrate to assess protease activity, aiming to circumvent limitations of the conventional casein-FITC assay (Huang et al., 2002; Nok, 2001). The new bioassay was integrated with liquid chromatography-mass spectrometry (LC-MS) methods to create a nanofractionation system for the simultaneous assessment of the bioactivity and identity of proteases present in snake venoms. The applicability of the platform was tested by profiling venoms of eight diverse viperid snake species.

2. Experimental

A Shimadzu UPLC system (SIL-30AC autosampler, DGU-20A degasser, LC30AD pumps, and SPD-M20A PDA detector) equipped with a C18 XBridge column (4.6 × 150 mm; 3.5 μm particle size) was used for LC separations. MS detection was performed using a MaXis HD qTOF instrument equipped with a standard ESI probe operating in positive mode (Bruker Daltonics, Bremen Germany). Greiner Bio-one black 384-well microtiter plates (Monroe, NC, USA) were used for collecting fractions and subsequent fluorescence experiments.

Lyophilized snake venoms were obtained from the Herpetarium of the Centre for Snakebite Research & Interventions at the Liverpool School of Tropical Medicine (UK) and from Latoxan (France). Snake venoms were from the following viper (Viperidae) species: *Calloselasma rhodostoma* (Malaysia), *Daboia russelii russelii* (Sri Lanka), *Echis carinatus* (India), *Echis coloratus* (Egypt), *Echis ocellatus* (Nigeria), *Echis pyramidum leakeyi* (Kenya), *Lachesis muta* (Costa Rica) and *Macrovipera lebetina* (Uzbekistan). These venoms were selected based on either their medical importance or to cover broad geographical distribution (e.g. worldwide coverage). Venoms were reconstituted in water and aliquots were stored at −80 °C before analysis and at −20 °C between analyses.

Rhodamine-110 bis-(p-tosyl-L-glycyl-L-prolyl-L-arginine amide) (referred to as rhodamine substrate) and leupeptin were purchased from ThermoFisher. Casein-FITC and solvents were purchased from Sigma-Aldrich. Milli-Q ultrapure water was obtained through an in-house Millipore filtration system. The fluorescence bioassay was conducted in phosphate buffer (PBS) (pH 7.4), which was also used to dilute substrate solutions. A ThermoFisher Varioskan plate reader with standard SkanIt software was used to record the fluorescence readout of the bioassay.

2.1. Fluorescence bioassay development

All fluorescence experiments were conducted in 384-well microtiter plates using the Varioskan plate reader. Measurements were performed at 37 °C, using an excitation wavelength of 485 nm and emission wavelength of 535 nm. The final volume of all wells was 50 μL. Crude venom was diluted in MilliQ water, while substrates were diluted in PBS (137 mM NaCl, 2.7 mM KCl, 10 mM Na_2HPO_4, 1.8 mM KH_2PO_4). To determine the minimum venom concentration required to observe protease activity, crude venom was diluted with MilliQ in series resulting in five experimental concentrations (33, 11, 4, 1 and 0.4 μg/mL). Of each venom concentration, 5 μL was added to 45 μL of PBS/substrate solution (10 μg/mL casein-FITC in PBS or 1 μM rhodamine substrate in PBS). The ensuing reaction was monitored by the plate reader for 15 min for either substrate. All venoms were assayed with both substrates. The appropriate/optimal substrate concentration required for the fluorescence bioassay was determined by measuring the fluorescence reaction rate for snake venoms in different starting concentrations with different substrate concentrations. Final casein-FITC substrate concentrations per well were 30, 10, and 5 μg/mL, and for the rhodamine substrate, final concentrations were 1, 500, and 100 nM. Of each casein-FITC substrate solution (300, 100, or 50 μg/mL) and rhodamine solution (10, 5, and 1 μM) 5 μL were incubated with 5 μL of crude snake venom (varyingrent concentrations) in 40 μL of PBS. The ensuing reactions were recorded for 15 min for all cases.

2.2. Nanofractionation system

The LC setup with parallel fractionation and MS detection used in this study was based on previously developed workflows (Mladic et al., 2016; Mladic et al., 2015). The eluent flow rate of 0.5 mL/min was controlled by two Shimadzu LC-30AD parallel pumps. Mobile phase A was made up of 98% water, 2% acetonitrile (ACN) and 0.1% formic acid (FA), and mobile phase B was 98% ACN, 2% water and 0.1% FA. The following LC gradient was applied: a linear increase from 0 to 50% B in 20 min, followed by a linear increase from 50% to 90% B in 4 min, followed by isocratic elution at 90% B for 5 min. Equilibration was achieved by a decrease from 90 to 0% B in 1 min followed by 10 min isocratic elution at 0% B. The column effluent was split in a 1 to 9 ratio diverting 10% of the flow to a PDA detector followed by the Q-TOF mass spectrometer. The remaining 90% of the UPLC eluent was collected as 6-s fractions in 384-well microtiter plates using a FractioMate™ (SPARK-Holland & VU, Netherlands, Emmen & Amsterdam) controlled by FractioMator software (Spark-Holland) or using an in-house built fraction collector based on a modified Gilson 235P autosampler controlled by in-house produced Ariadne software. MS data was acquired in positive mode from 50 to 3000 m/z using the following conditions: capillary voltage, 4500 V; nebulizer pressure, 0.4 Bar; dry gas flow, 4 L/min; dry gas temperature, 200 °C; collision cell energy, 6 eV; energy funnel 1 RF and multiple RF amplitudes, 400 V; quadrupole ion energy, 3 eV; collision RF, 1000 V.

Well plates with LC fractions were evaporated to dryness in a Christ RVC 2-33CDplus rotational vacuum concentrator and stored at −20 °C until assayed. Plates with fractionated venom were subjected to bioassays utilizing either the rhodamine or casein-FITC substrate. Both bioassays were performed by adding 50 μL substrate/buffer solution per well, followed by fluorescence measurement under the aforementioned plate reader conditions. The optimized concentrations of substrate per well were 10 μg/mL casein-FITC or 500 nM rhodamine substrate. Rhodamine substrate and casein-FITC reactions were monitored for 30 and 15 min, respectively. For each well, the slope of the increasing

fluorescence signal over time was plotted against the LC retention time of the probed fraction in order to generate a bioactivity chromatogram. Positive peaks in the obtained profile representing protease activity were correlated, with the parallel recorded UV and MS chromatograms allowing assignment of accurate molecular masses to active venom components.

3. Results and discussion

The aim of this project was to develop a fluorescence bioassay to detect individual proteases in snake venoms following chromatographic separation and fractionation. Studies relating to snake venom protease activity have traditionally relied on casein-based protease substrates such as casein-FITC (Arpitha et al., 2017; Borges et al., 2001; Choudhury et al., 2017; Cupp-Enyard, 2009; Delpierre, 1968; Mukherjee, 2008; Yee et al., 2016). This is partly because casein is widely available and targeted by a vast range of proteases, making it a generic substrate. However, when casein-FITC was used in the protease bioassay for measuring LC fractions of snake venoms, the background signal was very high and variable among assays (see Supporting Information Fig. S2). As a consequence, increases in fluorescence due to proteolytic cleavage of the substrate by venom proteases was largely obscured. We therefore investigated the potential of a rhodamine substrate to achieve lower background signals and better sensitivity for proteolytic toxins in snake venoms. First, the concentrations of venom and substrates were evaluated and optimized. Next, the performance of the casein-FITC and rhodamine substrates were compared. The optimal rhodamine-based protease bioassay, which showed to be superior to the FITC-based assy, was then applied to high-resolution LC fractions of venoms to and bioactivity chromatograms were constructed. These were used to correlate bioactivity of venom components with accurate masses obtained with MS detection parallel to fractionation.

As a critical note, we would like to mention that the original value of using a casein-FITC substrate is based in the variety of peptide bonds linked to the fluorescein label that are available for proteases; there are multiple fluorescein molecules chemically linked to casein via the reactive FITC molecule (i.e. chemically reactive fluorescein). This increases the likelihood of enzymatic cleavage by proteases regardless of specificity. Although the current rhodamine substrate only has two small peptides to be cleaved from its structure in order to form the fluorescent product and as such represents less variety in available peptide bonds to be cleaved, the small amino acid sequence of the attached peptides is anticipated to compensate for this by easy access of proteases to the peptide cleavage sites in the rhodamine substrate. This hypothesis is strengthened by other studies in which it was found that similar or the same substrate showed broad-range specificity for proteases (Cai et al., 2001; Grant et al., 2002; Kastrup et al., 2007; Klingel et al., 1994; Leytus et al., 1983; Zietek et al., 2018). This research showed the efficient and sensitive bioassaying of protease activity of several different crude venoms and of nanofractionated venom proteases. Although optimal protease activity cannot be expected for all SVMPs and SVSPs as it is not likely that the rhodamine substrate is a preferred substrate with optimal enzymatic kinetics for all venom proteases, it is expected that many proteases do convert the substrate at least to some extent.

3.1. Effect of venom and substrate concentration in protease bioassay

In order to compare casein-FITC, a conventional protease substrate, with the new rhodamine substrate, the minimum effective concentrations of each substrate, as well as the effect of crude venom concentration, were determined. This was achieved by incubating five concentrations (33, 11, 4.0, 1.0 and 0.4 μg/mL) of three crude snake venoms (*E. ocellatus, E. carinatus,* and *E. p. leakeyi*) with three concentrations of rhodamine substrate (1.0, 0.5 and 0.1 μM) or casein-FITC substrate (30, 10 and 5.0 μg/mL). Fig. 1 displays the fluorescence results obtained for each venom at five concentrations using the rhodamine substrate (for three concentrations) and the casein-FITC (at one concentration). High venom concentrations in combination with low substrate concentrations resulted in rapid substrate depletion which is difficult to monitor kinetically (i.e. full substrate conversion at low substrate concentration occurs too fast to profile). High substrate concentrations provided high background signals, obscuring the fluorescence signal increase upon substrate conversion at low venom concentrations.

When using 100 nM rhodamine substrate in the assay, only the highest venom concentration(s) (33 and/or 11 μg/mL) resulted in fluorescent signals that could be distinguished from the background. Still, at this low rhodamine substrate concentration, fluorescence intensity increase was minimal during the assay due to substrate depletion. When using high substrate and venom concentrations (i.e. 1000 nM and 33 μg/mL, respectively), intense fluorescence signals were obtained, but also high background signal. Moreover, consumption of substrate is significant. At a rhodamine substrate concentration of 500 nM, fluorescence signals were clearly distinguishable from baseline and the enzymatic reaction rates were sufficiently slow to be observed in the proper kinetic time window. Although the rhodamine substrate was somewhat more costly, casein-FITC was found to be a less sensitive fluorescence indicator of protease activity. The rhodamine substrate also showed a more generic applicability exhibiting clear protease activity towards all tested venoms, which was not the case for the casein-FITC substrate. The significant difference in sensitivity is shown in Fig. 1 (and in Fig. S1 for venoms of *Daboia russelii russelii*, *Echis coloratus* and *Lachesis muta*) demonstrating that the rhodamine-110-peptide substrate provides a clear advantage over casein–FITC.

3.2. Bioactivity profiling of LC-fractionated snake venoms

Casein-FITC (10 μg/mL) and the rhodamine substrate (500 nM) were also compared in bioassays applied to high-resolution venom fractions obtained after LC separation. Using casein-FITC, large signal to noise ratios were observed, resulting in protease activity being masked for most venoms (Fig. S2). Positive and negative control measurements (PBS + casein-FITC and PBS only, respectively) showed that casein-FITC by itself produces substantial fluorescence background (i.e. increase in fluorescence intensity in time), even in the absence of proteolytic conversion.

Using the rhodamine substrate for the same venom fractions, clear protease activity was observed for all venoms (Fig. S3). Regardless of the snake species, the bioactive venom proteases eluted within the 25–30 min elution window, although differences in fluorescence peak intensity and shape were observed between species. A representative result obtained for both substrates applied to the fractions of *E. ocellatus* is shown in Fig. 2. When using the rhodamine substrate, an increase in fluorescence slopes for wells containing eluted venom proteases was observed between 26 and 27 min. In wells without venom proteases, no substrate conversion occurred, as a constant baseline signal was observed (i.e. no slopes).

3.3. Assignment of bioactive venom proteases

The bioactivity profiles observed in the constructed bioassay chromatograms after LC fractionation were next correlated with mass data obtained by parallel MS detection. The bioactivity chromatograms were aligned with the UV and MS chromatograms taking delay times resulting from the flow volume to the fractionator into account. The positive peak/peaks in the bioactivity chromatograms, indicating protease activity, were correlated with peak shapes and retention times of peaks observed in the UV chromatogram and in the total ion chromatogram (TIC) by superimposing the chromatograms.

To identify accurate masses of bioactive components, we plotted the extracted ion chromatograms (XICs) that displayed peaks matching with the observed bioactivity peaks by shape and retention time. For

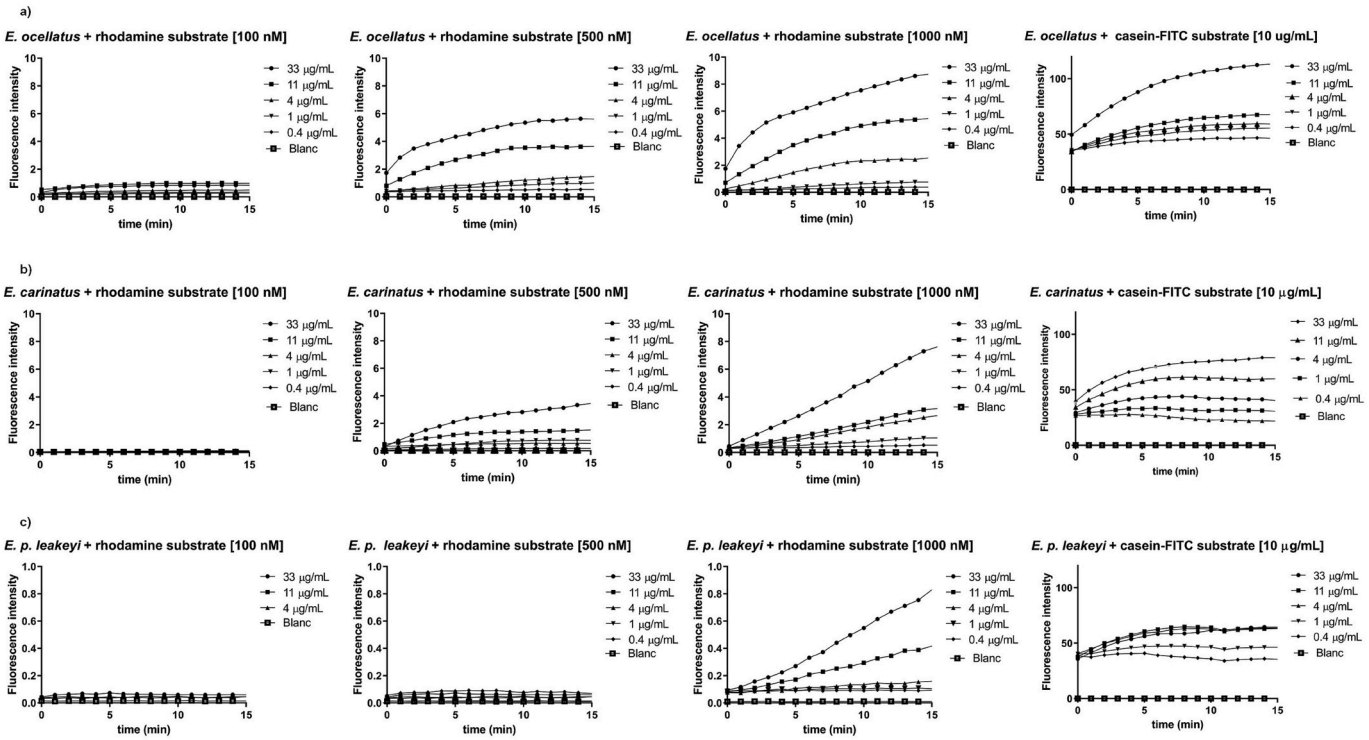

Fig. 1. Comparison of bioassay readouts between the rhodamine substrate and casein-FITC. Different concentrations of crude snake venoms (33, 1, 4, 1 and 0.4 µg/mL) were tested against three concentrations of rhodamine substrate (Column 1: rhodamine 100 nM; column 2: rhodamine 500 nM; column 3: rhodamine 1000 nM). A comparison was then made with the optimized casein-FITC (Column 4: 10 µg/mL) bioassay. Row (**a**) *Echis carinatus* Row (**b**) *Echis carinatus* and Row (**c**) Echis pyramidum leakeyi.

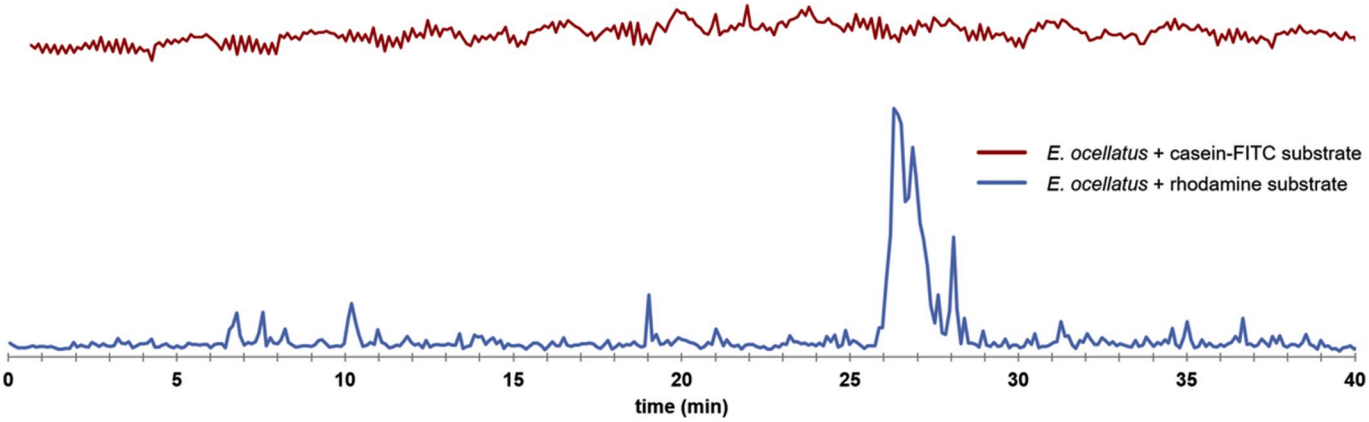

Fig. 2. Comparison of casein-FITC and rhodamine substrate bioassay readout. Red chromatogram: E. ocellatus + casein-FITC substrate; blue chromatogram: E. ocellatus + rhodamine substrate; X-axis: time (min). E. ocellatus venom was subjected to at-line nanofractionation after which the casein-FITC and rhodamine substrate bioassays were performed. Top: Fluorescence bioassay trace of nanofractionated E. ocellatus venom with casein-FITC substrate [10 µg/mL]. Bottom: Fluorescence bioassay trace of nanofractionated E. ocellatus venom with rhodamine substrate [500 nM]. (For interpretation of the references to color in this figure legend, the reader is referred to the Web version of this article.)

example, in Fig. 3 the peak for a component ion with a *m/z* of 2324.54 (charge state, 14+; deconvoluted mass, 30233 Da), nicely matched the detected bioactivity peak, indicating a venom protease. For the other venoms analyzed in this study, similar results were obtained (Fig. 4), showing the chromatographic window (20–30 min) in which the venom proteases elute.

The MS and UV chromatograms of the studied venoms, which are all from the family Viperidae, showed characteristic profiles that can be considered a fingerprint for each specific venom. This can be explained by variation in venom toxin composition being ubiquitous among snake species (Casewell et al., 2014; Slagboom et al., 2017; Tasoulis and Isbister, 2017). All of the studied snake species produce hemotoxic venoms rich in proteases, but the number of these toxins, their relative abundance, and the ratio of serine proteases to metalloproteases varies among the species (Casewell et al., 2009; Choudhury et al., 2017; Pahari et al., 2007; Sanz et al., 2008).

The additional detail observed in the UV and MS chromatograms reflects a number of venom components that are not visible in the bioassay (i.e. do not exhibit protease activity). The LC-UV data are particularly valuable as they allow comparison (i.e. correlation) with previous studies on the same snake venoms but in the context of other bioactivities. Several of the venoms studied here (*E. ocellatus*,

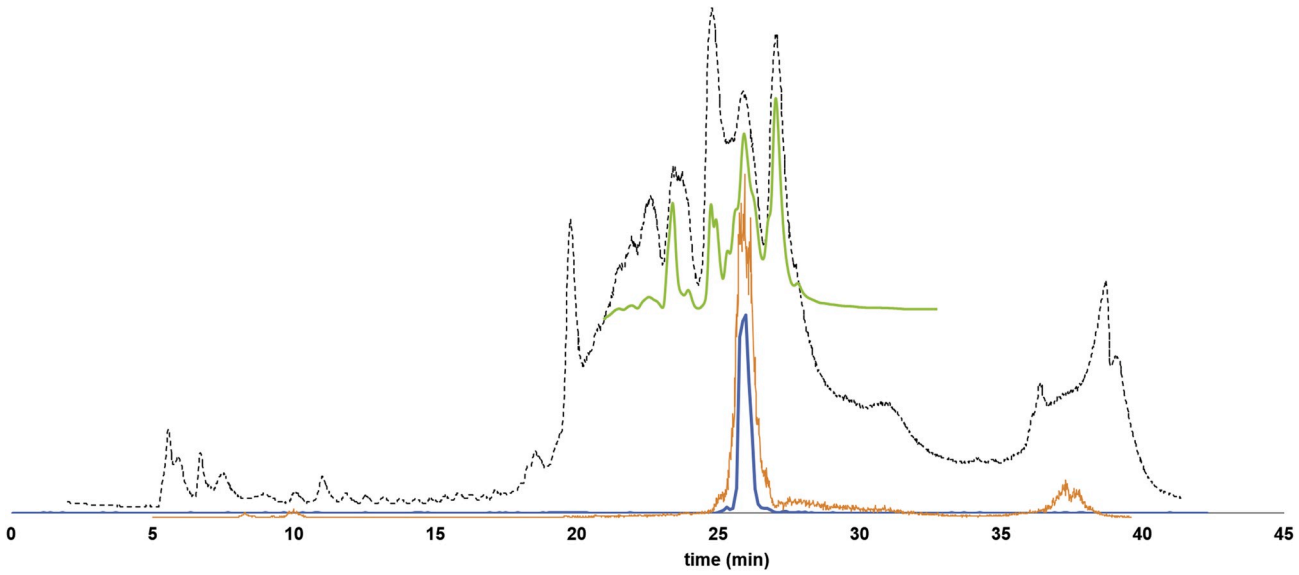

Fig. 3. Overlay of bioassay, UV and MS data. Fluorescence bioassay signal obtained with rhodamine substrate (blue), eXtracted Ion Chromatogram (XIC of m/z $2325{,}54^{+14}$ with an exact mass of 30233 Da; orange), UV trace (green; plotted only for the relevant time frame in which bioactivity was observed), and Total Ion Chromatogram (TIC; dotted black) traces of nanofractionated venom from *Lachesis muta*. X-axis: time (min). (For interpretation of the references to color in this figure legend, the reader is referred to the Web version of this article.)

Calloselasma rhodostoma and *Daboia russelli*) have recently been assessed by Slagboom et al. (2019) in order to establish the coagulopathic activities of venom toxins. This work included an in-depth identification study using accurate MS data in combination with bottom-up proteomics analysis of specific LC fractions. As Slagboom et al. used the same LC columns for venom separation, the LC-UV profiles of the venoms in the present and previous study could be readily compared and aligned. This allowed correlation of observed component peaks with mass and proteomics data previously obtained (Slagboom et al., 2019) and thus, identification of venom proteins responsible for the proteolytic bioactivities observed. The mass and proteomics data obtained by Slagboom et al. for the elution window where protease activities were observed, provided multiple protein identities, which are displayed in full in Table 1. The venom toxin IDs were obtained by a previously performed Mascot database search on species-specific databases generated from transcriptomic data and on the Swissprot/Uniprot database when no transcriptomic data was available for the species. For details on the Mascot database and search parameters, readers are referred to the study of Slagboom et al. (2019). The majority of the resulting assigned toxin classes are known to exhibit proteolytic activity, and include SVMPs and SVSPs. Although a number of other venom toxin types were also detected, these were found co-eluting with the identified proteases, suggesting that they are likely not contributing to the detected activites.

Evidence for this assertion is supported by the fact that these toxins were present at the same retention times as SVMPs and SVSPs. The toxins found in the area where protease activity was observed are tentative and each of these toxins can potentially exhibit the activity. However, suggestions based on the character of the toxin class can be made and in that sense the toxins that are most likely to be responsible for the activity are SVMPs and SVSPs. SVMPs and SVSPs are abundant in these species and are a main cause of venom-induced pathologies (Kini and Koh, 2016; Slagboom et al., 2017). For several of the bioactive peaks no clear corresponding XICs of m/z's indicative of proteases were found. Most likely, the concentrations of these proteases are below the online MS detection limit. This might be due to poor ionization efficiencies, which is particularly true for proteins with a molecular mass above 25 kDa.

4. Conclusions

This study describes the development of a rhodamine-110-peptide assay for profiling protease activity in both crude and LC fractionated venoms. Although it is considered the standard, the widely used casein-FITC substrate exhibits a significantly large background signal which resulted in low assay sensitivity and in the inability of integrating this substrate in nanofractionation analytics for post-column protease activity assying of low amounts of venom. The new rhodamine-110 based fluorescence bioassay developed here, was shown to be considerably more sensitive than the standard casein-FITC bioassay for the measurement of protease activity of viperid snake venoms in the nanofractionation set up. This is for example demonstrated in Fig. 2 where the casein-FITC based protease assay was unable to detect snake venom proteases due to the high background signal, while the rhodamine-110-substrate based assay showed clear bioactivity peaks.

In total eight viper venoms were profiled for active proteases using the new assay in conjunction with LC. The combination of constructed bioactivity chromatograms with online detected UV chromatograms is useful for comparing LC-UV-MS data obtained by one study with LC-UV-MS and bioassay data obtained by another as shown in this study where observed bioactivity was cross-linked with UV, MS and proteomics data from Slagboom et al. by using the same LC conditions. For several bioactive peaks in this study, concentrations of corresponding venom proteases were found to be too low to be detected by the TOF mass spectrometer used. However, MS identification was still possible by using bottom-up proteomics data obtained for bioactive fractions, indicating a number of different snake venom proteases. These findings underline the value of this novel assay for the detection of bioactive proteases from biological samples such as snake venoms. Moreover, we suggest that the approach described herein could be readily applied for the screening and selection of novel inhibitory molecules and/or antibodies for use as next generation treatments for snakebite (Ainsworth et al., 2018; Bulfone et al., 2018; Kini et al., 2018; Andreas H. Laustsen et al., 2018).

Declaration of competing interest

The authors declare that they have no known competing financial interests or personal relationships that could have appeared to influence

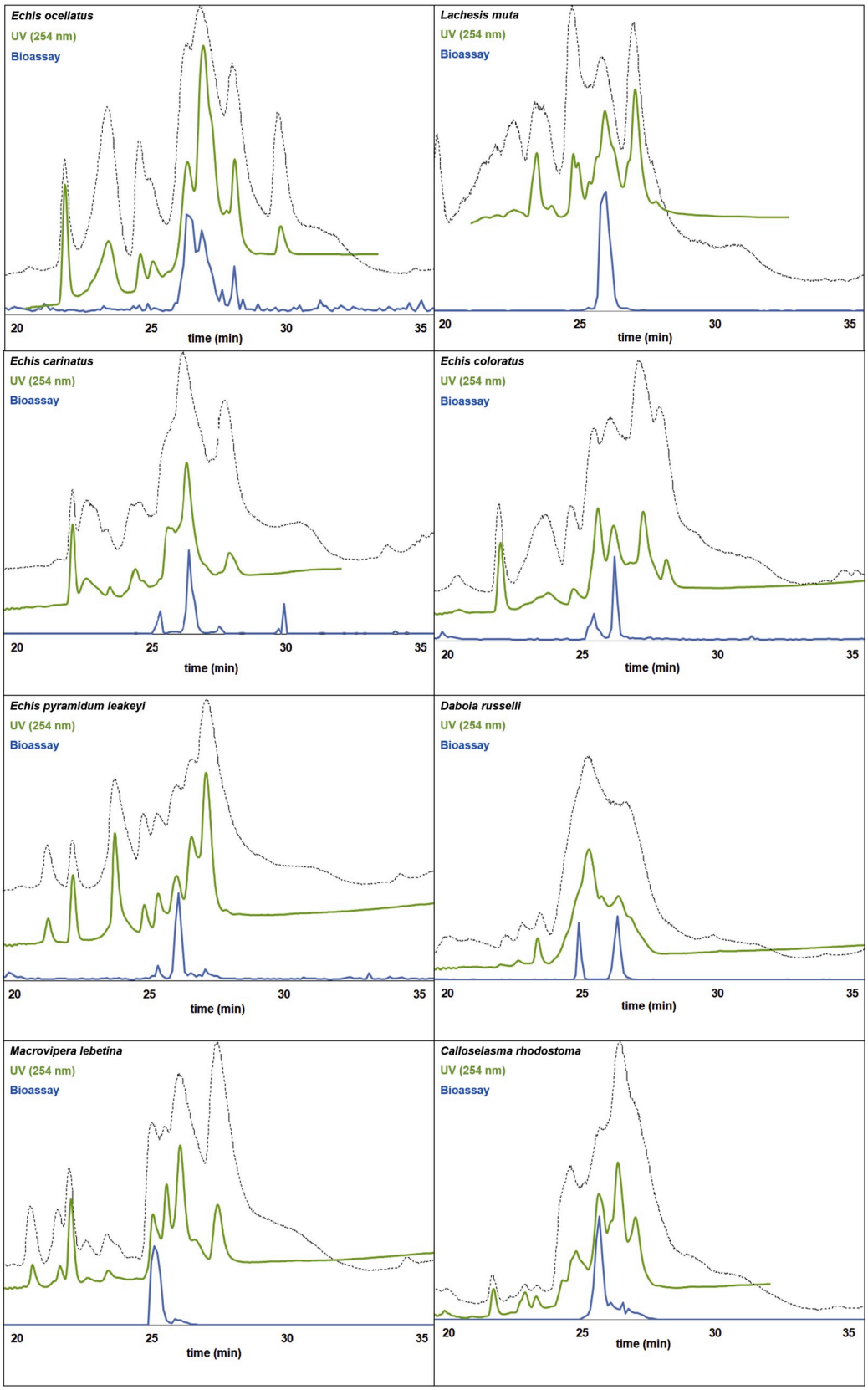

Fig. 4. Eight examples of time correlated MS, UV, and protease activity traces of nanofractionated venoms from different viperid species. Top left: Echis ocellatus; top right: *Lachesis muta*; second from top left: *Echis carinatus*; second from top right: Echis coloratus; second from bottom left: Echis pyramidium leakeyi; second from bottom right: *Daboia russelii*; bottom left: *Macrovipera lebetina*; bottom right: Calloselasma rhodostoma. The TIC and UV traces, top/black and middle/green respectively, were obtained concurrently during the fractionation of the same sample of venom which was subsequently subjected to the rhodamine bioassay to produce the fluorescence bioactivity trace shown in blue at the bottom of each figure. Traces were adjusted (aligned) according to the delay time between system components. (For interpretation of the references to color in this figure legend, the reader is referred to the Web version of this article.)

Table 1
Toxins found in the elution window where protease bioactivity was observed.

Species	Mascot results	Coverage %	Protein score	Toxin class
Echis ocellatus	Echis_ocellatus_EOC00022_83523635_SVMP	38	4511	SVMP
	Echis_ocellatus_04C11_EOC00015_PLA2	72	3117	PLA_2
	Echis_ocellatus_EOC00063_83523627_SVMP	29	1673	SVMP
	Echis_ocellatus_EOC00089_83523641_SVMP	26	966	SVMP
	Echis_ocellatus_EOC00404_83523645_SVMP	21	663	SVMP
	Echis_ocellatus_EOC00095_83523631_SVMP	9	558	SVMP
	Echis_ocellatus_01A10_EOC00265_CTL	48	424	CTL
	Echis_ocellatus_EOC00001_83523625_SVMP	8	310	SVMP
	Echis_ocellatus_EOC00013_83523633_SVMP	15	312	SVMP
	Echis_ocellatus_04F08_EOC00073_SVMP	22	272	SVMP
	Echis_ocellatus_03E06_EOC00140_PLA2	26	173	PLA_2
	Echis_ocellatus_04D06_EOC00087_CTL	9	75	CTL
	Echis_ocellatus_EOC00008_SVMP	5	66	SVMP
	Echis_ocellatus_03A04_EOC00167_LAAO	11	39	LAAO
	Echis_ocellatus_02C06_EOC00124_CTL	17	38	CTL
Calloselasma rhodostoma	VSPF1_CALRH	58	3658	SVSP
	SLEA_CALRH	68	3094	CTL
	PA2AB_CALRH	83	1315	PLA_2
	VSPF2_CALRH	53	952	SVSP
	VM1K_CALRH	33	607	SVMP
	VM2RH_CALRH	27	344	SVMP
	SLYA_CALRH	53	317	CTL
	SLEB_CALRH	43	201	CTL
	SLYB_CALRH	15	39	CTL
Daboia russelli russelli	Daboia_russelli_pulchella_1CL5_PLA2	79	2920	PLA_2
	Daboia_russelli_1Q6V_chain_A_PLA2	58	1193	PLA_2
	Daboia_russelli_CAA48457_1_PLA2	48	1052	PLA_2
	Daboia_russelli_siamensis_ADP88559_1_SVSP	11	120	SVSP
	Daboia_russelli_3SBK_SVSP	8	72	SVSP

the work reported in this paper.

CRediT authorship contribution statement

Coleen Neumann: Investigation, Writing - original draft. **Julien Slagboom:** Investigation, Writing - original draft, Software. **Govert W. Somsen:** Writing - review & editing. **Freek Vonk:** Software, Writing - review & editing. **Nicholas R. Casewell:** Writing - review & editing, Supervision. **Carmen L. Cardoso:** Software. **Jeroen Kool:** Writing - review & editing, Supervision.

Acknowledgements

Carmen L. Cardoso was financially supported by the São Paulo Research Foundation (FAPESP [grant number 2016-14482-5]). Nicholas R. Casewell acknowledges funding from a Sir Henry Dale Fellowship (200517/Z/16/Z) jointly funded by the Wellcome Trust and Royal Society.

Appendix A. Supplementary data

Supplementary data related to this article can be found at https://doi.org/10.1016/j.toxicon.2020.02.015.

References

Ainsworth, S., Slagboom, J., Alomran, N., Pla, D., Alhamdi, Y., King, S.I., Bolton, F.M.S., Gutiérrez, J.M., Vonk, F.J., Toh, C.-H., Calvete, J.J., Kool, J., Harrison, R.A., Casewell, N.R., 2018. The paraspecific neutralisation of snake venom induced coagulopathy by antivenoms. Commun. Biol. 1 (1), 34.

Arpitha, A., Santhosh, M.S., Rohit, A.C., Girish, K.S., Vinod, D., Aparna, H.S., 2017. Inhibition of snake venom metalloproteinase by β-lactoglobulin peptide from buffalo (Bubalus bubalis) colostrum. Appl. Biochem. Biotechnol. 182 (4), 1415–1432.

Borges, M.H., Soares, A.M., Rodrigues, V.M., Oliveira, F., Fransheschi, A.M., Rucavado, A., Giglio, J.R., Homsi-Brandeburgo, M.I., 2001. Neutralization of proteases from Bothrops snake venoms by the aqueous extract from Casearia sylvestris Flacourtiaceae). Toxicon 39, 1863–1869.

Bulfone, T.C., Samuel, S.P., Bickler, P.E., Lewin, M.R., 2018. Developing small molecule therapeutics for the initial and adjunctive treatment of snakebite. J. Trop. Med. 2018, 4320175.

Cai, S.X., Zhang, H.-Z., Guastella, J., Drewe, J., Yang, W., Weber, E., 2001. Design and synthesis of Rhodamine 110 derivative and Caspase-3 substrate for enzyme and cell-based fluorescent assay. Bioorg. Med. Chem. Lett 11 (1), 39–42.

Casewell, N.R., Harrison, R.A., Wüster, W., Wagstaff, S.C., 2009. Comparative venom gland transcriptome surveys of the saw-scaled vipers (Viperidae: Echis) reveal substantial intra-family gene diversity and novel venom transcripts. BMC Genom. 10, 564.

Casewell, N.R., Wagstaff, S.C., Wüster, W., Cook, D.A.N., Bolton, F.M.S., King, S.I., Pla, D., Sanz, L., Calvete, J.J., Harrison, R.A., 2014. Medically important differences in snake venom composition are dictated by distinct postgenomic mechanisms. Proc. Natl. Acad. Sci. Unit. States Am. 111 (25), 9205–9210. https://doi.org/10.1073/pnas.1405484111.

Chippaux, J.-P., Williams, V., White, J., 1991. Snake venom variability: methods of study, results and interpretation. Toxicon 29 (11), 1279–1303.

Choudhury, M., Suvilesh, K.N., Vishwanath, B.S., Velmurugan, D., 2017. EC-PIII, a novel non-hemorrhagic procoagulant metalloproteinase: purification and characterization from Indian Echis carinatus venom. Int. J. Biol. Macromol. 2018 (106), 193–199.

Cupp-Enyard, C., 2009. Use of the protease fluorescent detection kit to determine protease activity. JoVE 30, e1514.

Delpierre, G.R., 1968. Studies on african snake venoms—I the proteolytic activities of some african viperidae venoms. Toxicon 5 (4), 233–238.

Fry, B.G., Scheib, H., van der Weerd, L., Young, B., McNaughtan, J., Ramjan, S.F.R., Vidal, N., Poelmann, R.E., Norman, J.A., 2008. Evolution of an arsenal: structural and functional diversification of the venom system in the advanced snakes (Caenophidia). Mol. Cell. Proteomics: MCP 7 (2), 215–246.

Grant, S.K., Sklar, J.G., Cummings, R.T., 2002. Development of novel assays for proteolytic enzymes using rhodamine-based fluorogenic substrates. J. Biomol. Screen 7 (6), 531–540.

Gutiérrez, J.M., Calvete, J.J., Habib, A.G., Harrison, R.A., Williams, D.J., Warrell, D.A., 2017. Snakebite envenoming. Nat. Rev. Dis. Prim. 3, 17063.

Gutiérrez, J.M., Escalante, T., Rucavado, A., Herrera, C., 2016. Hemorrhage caused by snake venom metalloproteinases: a journey of discovery and understanding. Toxins 8 (4).

Hedstrom, L., 2002. Serine protease mechanism and specificity. Chem. Rev. 102 (12), 4501–4524.

Huang, K.-F., Chiou, S.-H., Ko, T.-P., Wang, A.H.-J., 2002. Determinants of the inhibition of a Taiwan habu venom metalloproteinase by its endogenous inhibitors revealed by X-ray crystallography and synthetic inhibitor analogues: inhibition of a SVMP by its endogenous inhibitors. Eur. J. Biochem. 269 (12), 3047–3056.

Kastrup, C.J., Shen, F., Runyon, M.K., Ismagilov, R.F., 2007. Characterization of the threshold response of initiation of blood clotting to stimulus patch size. Biophys. J. 93 (8), 2969–2977.

Kini, R.M., 2005. Serine proteases affecting blood coagulation and fibrinolysis from snake venoms. Pathophysiol. Haemostasis Thrombosis 34 (4–5), 200–204.
Kini, R.M., Koh, C.Y., 2016. Metalloproteases affecting blood coagulation, fibrinolysis and platelet aggregation from snake venoms: definition and nomenclature of interaction sites. Toxins 8 (10).
Kini, R.M., Sidhu, S.S., Laustsen, A.H., 2018. Biosynthetic oligoclonal antivenom (BOA) for snakebite and next-generation treatments for snakebite victims. Toxins 10 (12), 534.
Klingel, S., Rothe, G., Kellermann, W., Valet, G., 1994. Chapter 29 flow cytometric determination of cysteine and serine proteinase activities in living cells with rhodamine 110 substrates. In: Darzynkiewicz, Z., Paul Robinson, J., Crissman, H.A. (Eds.), Methods in Cell Biology, vol. 41. Academic Press, pp. 449–459.
Laustsen, A.H., Karatt-Vellatt, A., Masters, E.W., Arias, A.S., Pus, U., Knudsen, C., Oscoz, S., Slavny, P., Griffiths, D.T., Luther, A.M., Leah, R.A., Lindholm, M., Lomonte, B., Gutiérrez, J.M., McCafferty, J., 2018. In vivo neutralization of dendrotoxin-mediated neurotoxicity of black mamba venom by oligoclonal human IgG antibodies. Nat. Commun. 9 (1), 3928.
Leytus, S.P., Melhado, L.L., Mangel, W.F., 1983. Rhodamine-based compounds as fluorogenic substrates for serine proteinases. Biochem. J. 209 (2), 299–307.
Mladic, Marija, de Waal, Tessa, Burggraaff, Lindsey, Slagboom, Julien, Somsen, Govert W., Niessen, Wilfried M.A., Manjunatha Kin, R., Kool, Jeroen, 2017. Rapid screening and identification of ACE inhibitors in snake venoms using at-line nanofractionation LC-MS. Anal. Bioanal. Chem. 409 (25), 5987–5997.
Mladic, M., Scholten, D.J., Niessen, W.M.A., Somsen, G.W., Smit, M.J., Kool, J., 2015. At-line coupling of LC–MS to bioaffinity and selectivity assessment for metabolic profiling of ligands towards chemokine receptors CXCR1 and CXCR2. J. Chromatogr. B 1002, 42–53.
Mladic, M., Zietek, B.M., Iyer, J.K., Hermarij, P., Niessen, W.M.A., Somsen, G.W., Kini, R. M., Kool, J., 2016. At-line nanofractionation with parallel mass spectrometry and bioactivity assessment for the rapid screening of thrombin and factor Xa inhibitors in snake venoms. Toxicon 110, 79–89.
Mukherjee, A.K., 2008. Characterization of a novel pro-coagulant metalloprotease (RVBCMP) possessing α-fibrinogenase and tissue haemorrhagic activity from venom of Daboia russelli russelli (Russell's viper): evidence of distinct coagulant and haemorrhagic sites in RVBCMP. Toxicon 51 (5), 923–933.
Nok, A.J., 2001. A novel nonhemorragic protease from the African puff adder (Bitis arietans) venom. J. Biochem. Mol. Toxicol. 15 (4), 215–220.
Pahari, S., Mackessy, S.P., Kini, R.M., 2007. The venom gland transcriptome of the Desert Massasauga Rattlesnake (Sistrurus catenatus edwardsii): towards an understanding of venom composition among advanced snakes (Superfamily Colubroidea). BMC Mol. Biol. 8, 115.
Sanz, L., Escolano, J., Ferretti, M., Biscoglio, M.J., Rivera, E., Crescenti, E.J., Angulo, Y., Lomonte, B., Gutiérrez, J.M., Calvete, J.J., 2008. Snake venomics of the South and Central American Bushmasters. Comparison of the toxin composition of Lachesis muta gathered from proteomic versus transcriptomic analysis. J. Proteomics 71 (1), 46–60.
Schauperl, M., Fuchs, J.E., Waldner, B.J., Huber, R.G., Kramer, C., Liedl, K.R., 2015. Characterizing protease specificity: how many substrates do we need? PloS One 10 (11).
Slagboom, J., Kool, J., Harrison, R.A., Casewell, N.R., 2017. Haemotoxic snake venoms: their functional activity, impact on snakebite victims and pharmaceutical promise. Br. J. Haematol. 177 (6), 947–959.
Slagboom, J., Mladić, M., Xie, C., Vonk, F., Somsen, G.W., Casewell, N.R., Kool, J., 2019. High Throughput Screening and Identification of Coagulopathic Snake Venom Proteins and Peptides Using Nanofractionation and Proteomics Approaches. BioRxiv, 780155.
Tasoulis, T., Isbister, G.K., 2017. A review and database of snake venom proteomes. Toxins 9 (9).
Yee, K.T., Pitts, M., Tongyoo, P., Rojnuckarin, P., Wilkinson, M.C., 2016. Snake venom metalloproteinases and their peptide inhibitors from Myanmar Russell's viper venom. Toxins 9 (1).
Zietek, B.M., Mayar, M., Slagboom, J., Bruyneel, B., Vonk, F.J., Somsen, G.W., Casewell, N.R., Kool, J., 2018. Liquid chromatographic nanofractionation with parallel mass spectrometric detection for the screening of plasmin inhibitors and (metallo)proteinases in snake venoms. Anal. Bioanal. Chem. 410 (23), 5751–5763.